

# A New (Trifluoromethane)Sulfonylimide Single-Ion Conductor with PEG Spacer for All-Solid-State Lithium-Based Batteries

Published as part of ACS Materials Letters special issue "Post-Lithium Battery Materials".

Gabriele Lingua,<sup>▽</sup> Vladislav Y. Shevtsov,<sup>▽</sup> Petr S. Vlasov, Laura Puchot, Claudio Gerbaldi,\* and Alexander S. Shaplov\*



Cite This: *ACS Materials Lett.* 2024, 6, 5429–5437



Read Online

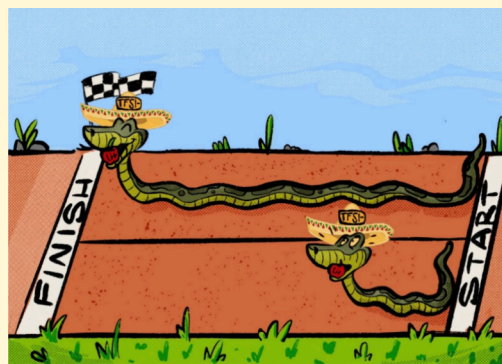
ACCESS |

Metrics & More

Article Recommendations

Supporting Information

**ABSTRACT:** The choice of ionic-liquid-like monomers (ILM) for single-ion conducting polyelectrolytes (SICPs) is crucial for the performance of all-solid-state lithium batteries. In the current study, we propose a novel approach for development of SICPs via design and synthesis of a new ILM with long poly(ethylene oxide) spacer between methacrylic group and (trifluoromethane)sulfonylimide anion. Its homopolymer shows an ionic conductivity that is  $\sim 5$  orders of magnitude higher ( $9.2 \times 10^{-8} \text{ S cm}^{-1}$  at 25 °C), in comparison with previously reported analogues, while the conductivity of its random copolymer with poly(ethylene glycol)methyl ethermethacrylate reaches the levels of  $10^{-6}$  and  $10^{-5} \text{ S cm}^{-1}$  at 25 and 70 °C, respectively. The copolymer provides excellent thermal ( $T_{\text{onset}} \approx 200 \text{ °C}$ ) and electrochemical (4.5 V vs Li<sup>+</sup>/Li) stabilities, good compatibility with Li metal, and effective suppression of dendrite growth. Li/SICP/LiFePO<sub>4</sub> cells are capable of reversibly operating at different C rates, demonstrating excellent Coulombic efficiency and retaining specific capacity upon prolonged charge/discharge cycling at a relatively high current rate (C/5) at 70 °C.



Single-ion-conducting polyelectrolytes (SICPs) are a relatively new subclass of solid-state polymer electrolytes (SPEs) that have the potential to revolutionize solid-state lithium-based batteries industry, enabling safe operation of Li metal anode in future truly solid-state Li-metal batteries (LiMBs).<sup>1,2</sup> Structurally, SICP is a polyelectrolyte having anionic moieties covalently attached to the polymer backbone and lithium counterions that are free to move.

Although SICPs are known from the early 1980s,<sup>3</sup> the real breakthrough was gained in the middle of 2010s with the application of ionic liquids (ILs) chemistry and (trifluoromethane)sulfonylimide (TFSI) anion,<sup>4–7</sup> in particular. The introduction of anions with high delocalization and low basicity allowed for the increase of overall ionic conductivity in SICPs, generally approaching the level of  $10^{-7}$ – $10^{-6} \text{ S cm}^{-1}$  at 25 °C.<sup>1,2</sup> Similar to SPEs, SICPs offer high thermal stability, nonvolatility, high electrochemical stability, and prevent any risks of liquid electrolyte leakage outside the battery case.<sup>8</sup> Moreover, since anions in SICPs are chemically bonded to the main backbone, their mobility is limited and only the Li<sup>+</sup> cation will contribute to a permanent flow of charge, thus increasing the Li ion transference number

( $t_{\text{Li}^+}$ ) close to unity.<sup>9</sup> This is expected to prevent the concentration gradients (polarization), thus contributing to circumvent (at least limit) dendrite growth at the surface of the Li metal anode in LiMBs.

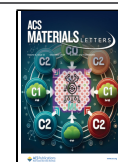
Despite extensive research efforts,<sup>1,2,10</sup> a competitive LiMB utilizing SICP electrolyte that satisfies industrial process needs and meets the market requirements for modern, high energy/power density batteries has yet to be developed. One of the reasons is connected with the insufficient ionic conductivity of SICPs being below that of salt-in-PEO polymer electrolytes ( $4 \times 10^{-5}$ – $9 \times 10^{-4} \text{ S cm}^{-1}$  at 25 °C).<sup>11</sup> Three approaches to overcome this problem have been suggested: (a) synthesis of cross-linked SICPs plasticized with polar organic additives (see, for example, refs 5 and 12–16); (b) preparation of

Received: August 13, 2024

Revised: November 3, 2024

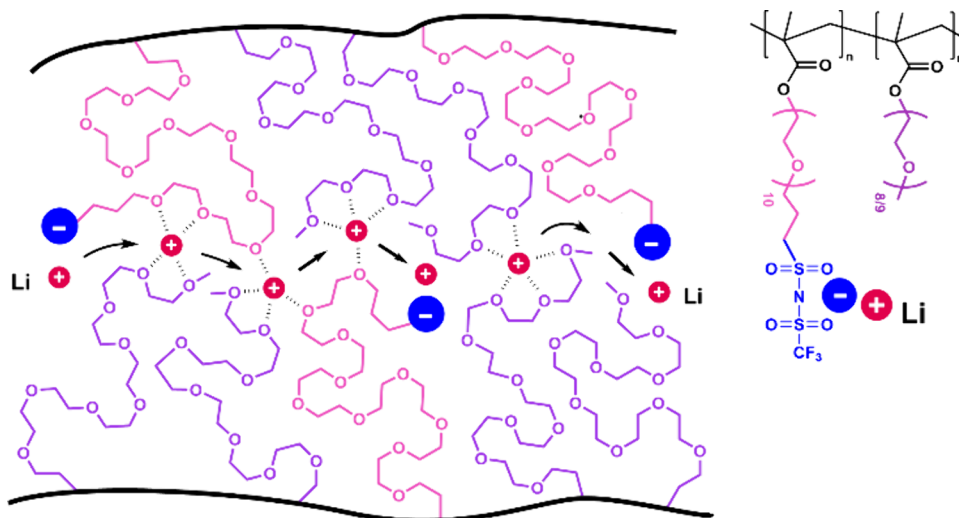
Accepted: November 4, 2024

Published: November 15, 2024





**Scheme 2. Structure of Single-Ion Conducting Polymer Electrolytes (SICPs) Developed in the Present Study and the Proposed Route for Li<sup>+</sup> Cation Mobility**



for SICPs based on LiMTFSI and **11**, respectively.<sup>25</sup> The last breakthrough was achieved by the group of Vidal et al. via synthesis of ILM **12** (Scheme 1 and Table S1, entry 14).<sup>32,33</sup> When combined with 1-methyl-3-ethyl imidazolium cation the polymerization of **12** produced SICP with as high conductivity as  $6.5 \times 10^{-4} \text{ S cm}^{-1}$  (25 °C). However, the presence of a urea linkage as well as the direct bonding of negatively charged nitrogen to a carbon atom will significantly reduce the electrochemical stability of the respective SICP and will not allow its utilization in LIBs.

Analyzing the structures of ILMs presented in Scheme 1, it can be concluded that the following structural parameters in ILMs are supposed to enhance the ionic conductivity of respective SICPs: (a) the introduction of sufficiently long spacers between the polymer backbone and the chemically attached anion; (b) the presence of the polar ethylene oxide units; and (c) the exception of electrochemically unstable groups in the spacer. Taking this into account, in this work, we developed a new ionic monomer (Scheme 1, **13**), where the methacrylic moiety and TFSI anion are separated by a long and flexible PEG linker. The synthesized monomer, denoted as TBAM(PEG)TFSI, was then homo- and copolymerized with PEGM via simple free radical polymerization (Scheme 2). After the exchange to Li<sup>+</sup>, all SICPs were thoroughly investigated in terms of their thermal, rheological, and electrochemical behavior. Furthermore, the best-performing SICP was used as a truly solid-state electrolyte in lab-scale Li-metal cells. Finally, it was demonstrated that the newly prepared SCIP based on LiM(PEG)TFSI outperformed the previously reported LiMTFSI- and LiMESTTFSI-derived polyelectrolytes, most notably, in terms of ionic conductivity, specific capacity retention, and rate capability at high charge/discharge regimes in battery cells.

## ■ SYNTHESIS OF IONIC LIQUID MONOMER TBAM(PEG)TFSI

For full details/description/acronyms of materials and methods, the reader is referred to the Supporting Information (SI) file. The synthetic pathway for the preparation of TBAM(PEG)TFSI monomer (Scheme 3), its <sup>1</sup>H, <sup>13</sup>C, HSQC, and <sup>19</sup>F NMR and IR spectra (Figures S2–S6), high-

resolution mass spectra (Figure S7), and elemental analysis are presented in the SI file. The synthesized TBAM(PEG)TFSI has a number-average molecular weight ( $M_n$ ) of 848.94 au with the molecular dispersity index ( $\mathcal{D}$ ) of 1.030 and represents a viscous light-yellow liquid with a glass-transition temperature ( $T_g$ ) of −63 °C.

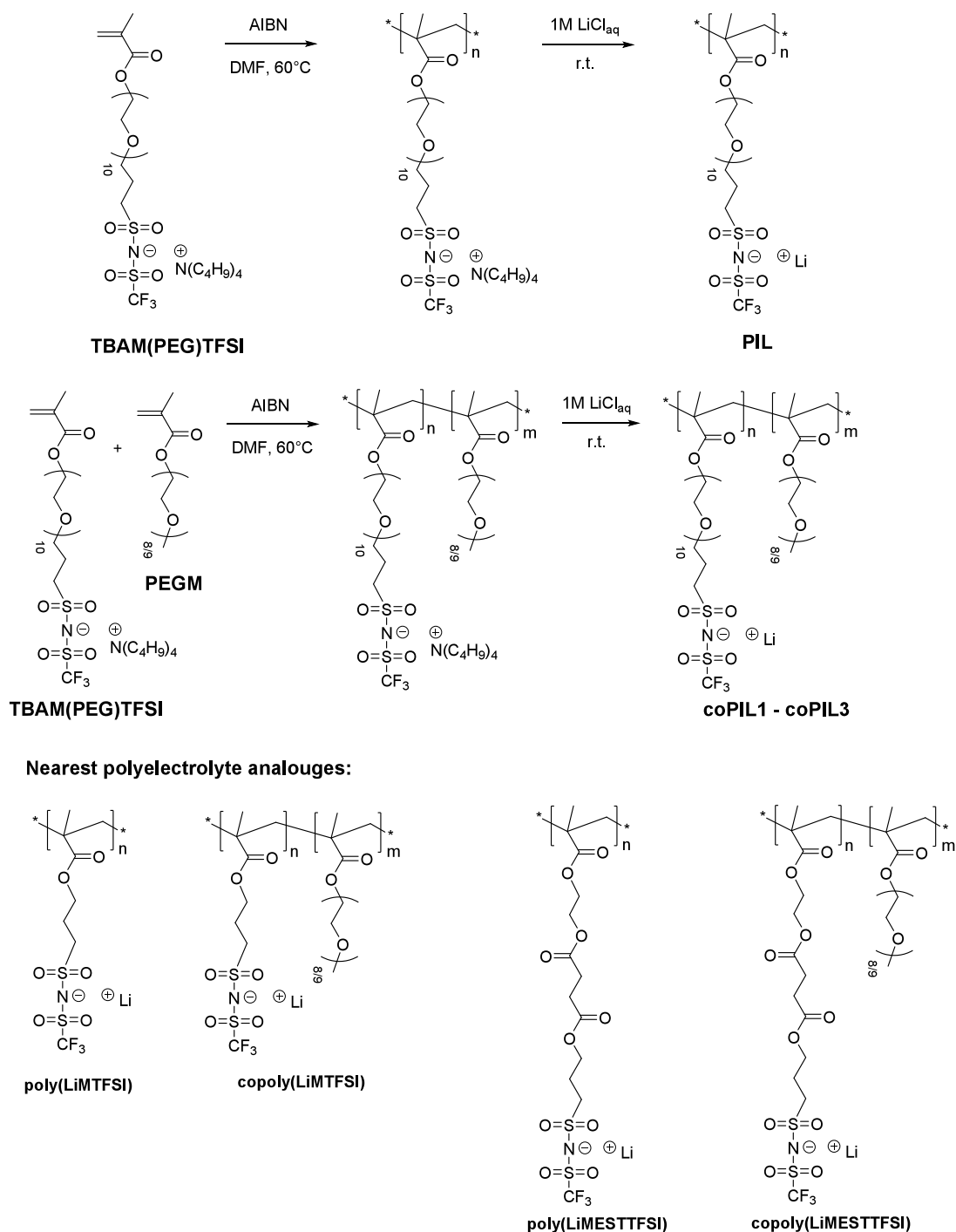
## ■ FREE RADICAL HOMOPOLYMERIZATION AND COPOLYMERIZATION OF TBAM(PEG)TFSI

The homopolymer of TBAM(PEG)TFSI was prepared via simple free-radical polymerization initiated by AIBN in DMF solution and denoted as PIL (Scheme 3). In addition, three copolymers of TBAM(PEG)TFSI with PEGM were synthesized in a similar manner by random copolymerization in three different ratios (coPIL1–coPIL3). GPC in a 0.1 M LiTFSI solution in DMF was used to investigate the molecular weights and the  $M_w/M_n$  ratios of the obtained polyelectrolytes. As can be seen from Table 1, for all polymers, the determined  $M_n$  values were relatively high, ranging from 62 kDa to 86 kDa. The obtained polymers represented soft yellow waxlike materials, that can easily form coatings, but not the self-standing films. Afterwards, all four polymers underwent ion exchange to substitute tetrabutyl ammonium cation with the Li one. Polyelectrolyte structures and purity were confirmed by <sup>1</sup>H, <sup>7</sup>Li, and <sup>19</sup>F NMR and IR spectroscopy (see Figures S9–S15).

## ■ IONIC CONDUCTIVITY MEASUREMENTS

Ionic conductivity ( $\sigma_{DC}$ ) as a function of temperature (Figure 1) for PIL and coPILs was investigated by using electrochemical impedance spectroscopy (EIS). The obtained values for PIL and coPIL1–coPIL3 were further compared to the nearest analogues, namely, poly(LiMTFSI) and poly(LiMESTTFSI) (Scheme 3 and Table 1). Notably, PIL demonstrated significantly improved ionic conductivity when compared to its predecessors poly(LiMTFSI) and poly(LiMESTTFSI), namely,  $9.2 \times 10^{-8} \text{ S cm}^{-1}$  against  $1.1 \times 10^{-12} \text{ S cm}^{-1}$  (ref 22) and  $<10^{-11} \text{ S cm}^{-1}$  (ref 25) at 25 °C, respectively (see Table 1). These results indicate that the introduction of the long oxyethylene spacers significantly improves the mobility of the polymer side chains, facilitating

**Scheme 3.** Synthesis of SICPs Based on M(PEG)TFSI Monomer with Li Cations and Their Nearest Polyelectrolyte Analogues<sup>22,25</sup> Used for Comparison



the Li cation coordination, resulting in the overall increase of ionic conductivity of PIL (Figure 1). The copolymerization of TBAM(PEG)TFSI with PEGM and subsequent ion exchange to Li cations allowed to further improve the ionic conductivity of the resulting SICPs by nearly 1.5 orders of magnitude at 25 °C (Table 1 and Figure 1).

Thus, it can be concluded that either the length of the PEG spacer equal to 10 EO units is not sufficient to fully solubilize Li cations or that the presence of side dangling PEG chains is pivotal to dilute chemically bonded TFSI anions, to effectively surround Li cations, and to establish their perfect transfer. The

greatest boost in ionic conductivity of coPIL was achieved when 2 PEGM molar equivalents were taken with respect to 1 mol equiv of TBAM(PEG)TFSI, resulting in  $\sigma$  values as high as  $3.0 \times 10^{-6} \text{ S cm}^{-1}$  at 25 °C (Table 1). The combination of synthesized PEG-based monomer with PEGM provided 1 order of magnitude higher ionic conductivity compared to copolymers with alkyl and ester spacers (i.e.,  $2.3 \times 10^{-7} \text{ S cm}^{-1}$  (ref 22) and  $1.2 \times 10^{-7} \text{ S cm}^{-1}$  (ref 25) at 25 °C, respectively, for copoly(LiMTFSI) and copoly(LiMESTTFSI), respectively; see Scheme 3).



Table 1. Selected Properties of SICPs Prepared by Free Radical (Co)polymerization

polymer	$M_n$ (SEC) <sup>a</sup> (g mol <sup>-1</sup> )	$M_w/M_n$ (SEC) <sup>a</sup>	[ILM]/[PEGM]		yield (%) <sup>c</sup>	$\sigma_{DC}$ (S cm <sup>-1</sup> )		$T_g^d$ (°C)	$T_{onset}^e$ (°C)
			theoretical molar ratio	experimental ratio <sup>b</sup>		25 °C	70 °C		
PIL	61900	1.9	—	—	78	$9.2 \times 10^{-8}$	$9.8 \times 10^{-6}$	-14	205
coPIL1	79500	5.5	1:1	1:1.1	76	$1.2 \times 10^{-6}$	$3.1 \times 10^{-5}$	-15	—
coPIL2	83900	5.6	1:2	1:2.8	74	$3.0 \times 10^{-6}$	$3.8 \times 10^{-5}$	-46	200
coPIL3	85900	5.8	1:4	1:4.6	76	$1.2 \times 10^{-6}$	$1.8 \times 10^{-5}$	-50	200
poly(LiMTFSI) <sup>f</sup>	52700	1.2	—	—	—	$1.1 \times 10^{-12}$	—	105	250
poly(LiMESTTFSI) <sup>f</sup>	1050000	3.1	—	—	—	$<10^{-11}$	—	18	225

<sup>a</sup>By GPC in 0.1 M solution of LiTFSI in DMF at 50 °C with PMMA standards. <sup>b</sup>By <sup>1</sup>H NMR (in DMSO-*d*<sub>6</sub>), calculated using eq S3 in the SI file.

<sup>c</sup>Isolated yield. <sup>d</sup>By DSC at a rate of 5 °C/min. <sup>e</sup>Onset weight loss temperature by TGA. <sup>f</sup>For comparison from refs 22 and 25.

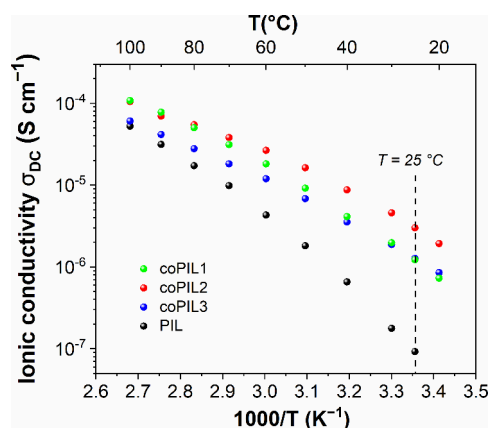


Figure 1. Ionic conductivity versus temperature (from 20 °C to 100 °C) plots for PIL and coPILs.

For both PIL and coPIL1–coPIL3 (Figure 1), the temperature dependence of ionic conductivity was not fully linear, thus deviating from Arrhenius' law (Figure 1). In contrast, the inverse temperature dependence of  $\sigma_{DC}$  followed a typical Vogel–Fulcher–Tammann (VFT) behavior for all studied PILs. The experimental results were thus fitted with the VFT equation, and the ionic conductivity activation energies ( $E_a$ ) for SICPs are listed in Table S2. All investigated samples demonstrated  $E_a$  values in the range of quasi- or truly SICPs.<sup>34,35</sup> The  $E_a$  values before and after 50 °C were extrapolated to carefully investigate the effect of the –EO– units in the homopolymer and the outcome of the addition of –EO– units by copolymerization with PEGM. As reported in Table S2, the  $E_a$  of a homopolymer drastically changes above 50 °C, decreasing from 20.91 kJ mol<sup>-1</sup> to 12.86 kJ mol<sup>-1</sup>. In contrast, for copolymers coPIL1–coPIL3, this difference was found to be less pronounced. Such a sharp change in  $E_a$  for PIL could be related to the intrinsic mobility of the –EO– segments of the polymer repeating unit, where the increase of the temperature above 50 °C can facilitate the Li ion hopping through TFSI anion sites, along with the decrease in the activation energy barrier of the conduction mechanism. The small addition of PEGM in coPIL1 allowed us to decrease the  $E_a$ , while further increases in PEGM content (coPIL2 and coPIL3) leads to an increase of  $E_a$ . It was assumed that such visible alteration in  $E_a$  values can be assigned to the change of the ionic conduction mechanism, which, in the case of coPIL2 and coPIL3, is governed prevalently by –EO– coordination. Thus, the limited quantity of PEGM in coPIL1 allows us to increase the side chain mobility, along with reducing the  $E_a$  without altering the ion conduction mechanism based on Li<sup>+</sup>

hopping between TFSI sites. Further addition of nonionic component is useful to decrease the  $T_g$  value of the copolymer and increase the ionic conductivity at low temperature; but, at the same time, it is affecting the ion conduction mechanism, leading to higher  $E_a$  values.

## THERMAL CHARACTERIZATION

The  $T_g$  values of polyelectrolytes (Figures S17 and S18) were determined by differential scanning calorimetry (DSC) and are reported in Table 1. Interestingly, PIL showed a  $T_g$  value of -14 °C, which is significantly lower than the  $T_g$  values of the previously synthesized SICP competitors, namely, 105 and 18 °C reported for poly(LiMTFSI) and poly(LiMESTTFSI), respectively (Table 1). It is evident that the short alkyl linker in LiMTFSI drastically hinders the mobility of the side chains of the resulting macromolecules, whereas the introduction of the long flexible spacer composed of EO units enhances the mobility of the side chains and overall reduces the polymer  $T_g$ . As both PIL and poly(LiMESTTFSI) are amorphous polymers and there is no influence of crystallinity, the presence of the sp<sup>2</sup>-hybridized carbon in ester segments of poly(LiMESTTFSI) renders them significantly more rigid, which results in a higher  $T_g$  in comparison with that of PIL having ether segments in the side chains. CoPIL1 demonstrated a  $T_g$  value that was almost identical (-15 °C) to that of pristine PIL. Most likely, in this case, the  $T_g$  decreasing effect of PEGM was attenuated by the already low  $T_g$  of the homopolymer, making it necessary to introduce a relatively high amount of comonomer to observe a considerable change. Indeed, further dilution with PEGM resulted in a dramatic decrease in  $T_g$ , as displayed by coPIL2 and coPIL3 (-46 and -49 °C, respectively).

The thermal degradation behavior was studied via TGA in air. The onset weight temperatures for PIL and coPIL2 were found to be 205 and 200 °C, respectively (Table 1). The weight loss profile of PIL revealed a one-step degradation mechanism, while two steps can be seen on the TGA curve of coPIL2 (Figure S19).

## RHEOLOGICAL CHARACTERIZATION

Given its highest ionic conductivity across the whole range of examined temperatures, coPIL2 was selected for further rheological studies in a small amplitude oscillatory flow mode at 25 and 70 °C, and the observed properties were compared with those of copoly(LiMTFSI). Figure S20 shows the evolution of the complex viscosity of coPIL2. At 1 Hz, the complex viscosity decreased from 750 mPa s to 156 mPa s when tested at 25 and 70 °C, respectively. At both temperatures, the complex viscosity decreased almost linearly

with the frequency. Figures S20b and S20c show the variation of loss and storage moduli as a function of the frequency at 25 and 70 °C for **coPIL2** and the copoly(**LiMTFSI**) as the reference with the same PEGM:ionic monomer molar ratio of 2:1. The loss modulus was higher than the storage modulus at both temperatures, accounting for the domination of the viscous over the elastic contribution; it is characteristic of an un-cross-linked polymer in a liquid or molten-like state over the entire frequency range. Although both copolymers exhibited viscous behavior, the **coPIL2** demonstrated storage and loss moduli that were 2 orders of magnitude higher than those observed in the range of explored frequencies, thus showing significantly better mechanical properties, in comparison with known copoly(**LiMTFSI**) analogue.<sup>22</sup>

### ■ ELECTROCHEMICAL STABILITY, Li TRANSFERENCE NUMBER, AND COMPATIBILITY WITH LITHIUM METAL

The evaluation of the electrochemical stability window (ESW) is particularly important to establish the voltage range at which the electrolyte can operate without undergoing unwanted degradation processes, which may account for performance decay during battery cycling. The ESW of **coPIL2** was evaluated by cyclic voltammetry (CV) at 70 °C in two distinct laboratory-scale lithium-metal cells, where **coPIL2** was in contact with Li foil and Cu metal electrode or carbon-coated Al electrode for the cathodic and anodic scans, respectively. The voltage window was scanned from the open circuit voltage (OCV) to −0.5 V and from the OCV to 5.0 V vs  $\text{Li}^+/\text{Li}$  redox potential for cathodic and anodic scans separately. The resulting profiles are shown in Figure S21. The anodic breakdown potential approached 4.5 V vs  $\text{Li}^+/\text{Li}$ , while, in cathodic scans, the profiles are reversible and, as expected, only two well-defined peaks were observed between −0.5 and 0.5 V vs  $\text{Li}^+/\text{Li}$ , which accounts for highly reversible lithium plating/stripping processes, thus confirming the efficient transfer of  $\text{Li}^+$  ions through the polymer network.

The lithium-ion transference number ( $t_{\text{Li}^+}$ ) of **coPIL2** was evaluated at 70 °C by methods that have been reported by both Evans–Vincent–Bruce<sup>36</sup> and Abraham et al.,<sup>37</sup> housing the electrolyte in a symmetrical cell with **Li/coPIL2/Li** configuration. Results from EIS and polarization current variation analysis are shown in Figures S22 and S23. The  $t_{\text{Li}^+}$  value was calculated to be equal to 0.96 (or 0.98, considering only the changes in the bulk resistance and applying the Evans–Vincent–Bruce equation). Moreover, the  $t_{\text{Li}^+}$  of the novel SICP is higher, compared to that of poly(PEGM-*b*-**LiMTFSI**) and poly[(**LiMTFSI**)-*b*-PEO-*b*-(**LiMTFSI**)] (0.83 (from ref 5<sup>5</sup>) and 0.91 (from ref 23), respectively). Based on the above-reported results, we can speculate that the −EO− fragments of the spacer in the ILM actively participate in the coordination of  $\text{Li}^+$  cations, resulting in enhanced mobility and transport.

Furthermore, the stability of **coPIL2** at the Li metal electrode interface (Figure S24) was investigated by means of reversible constant current (galvanostatic) Li plating and stripping test performed at 70 °C at different current densities, ranging from 0.10 to 0.50  $\text{mA cm}^{-2}$  (30 min per step). As shown in Figure S24, **coPIL2** demonstrated excellent stability during reversible plating and stripping, even at high current regimes without abnormal voltage drifts and any observable short circuit issues. Moreover, as shown in Figure S25, the resistance of the cell changed only slightly during the initial

stabilization period at the beginning of the experiment and became fully stable after 21 days.

### ■ ELECTROCHEMICAL BEHAVIOR IN A LABORATORY-SCALE LITHIUM METAL CELL

The **coPIL2** was further assembled in laboratory-scale lithium-metal cells, and its performance was evaluated in a **Li/coPIL2/LFP** configuration with  $\text{LiFePO}_4$  (LFP) as the positive electrode. The cell was tested at 70 °C at different current rates, denoted as  $C/n$ . As shown in Figure 2a, the first cell was

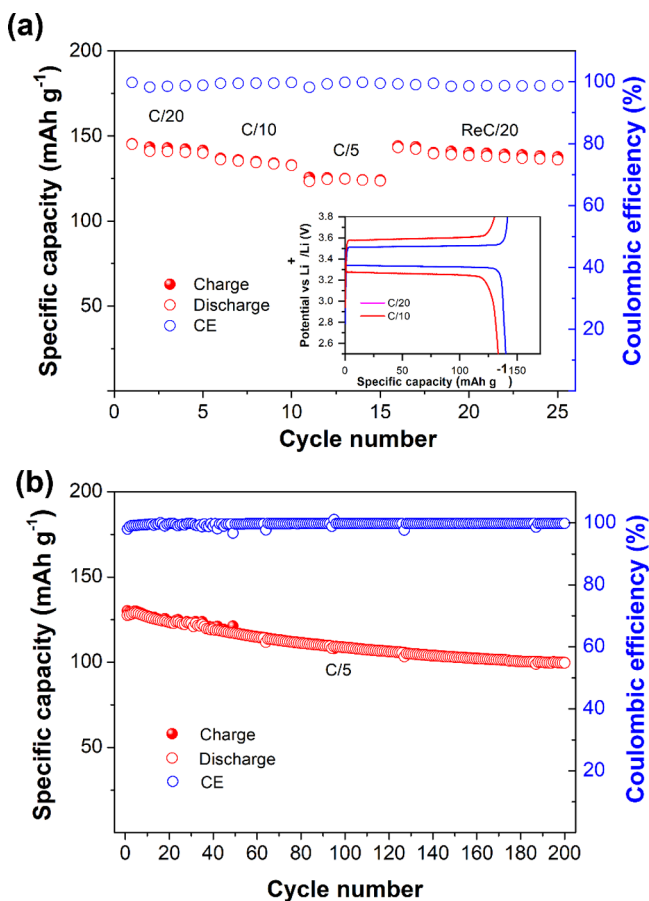


**Figure 2.** Galvanostatic cycling behavior of **Li/coPIL2/LFP** solid-state cells at 70 °C. Specific capacity versus cycle number dependence (a) with corresponding charge/discharge voltage versus specific capacity profiles in the inset and (b) specific capacity versus cycle number dependence at  $C/5$  upon prolonged cycling.

cycled starting from relatively low current of 15.7  $\mu\text{A}$  ( $C/20$ ) and up to 63.9  $\mu\text{A}$  ( $C/5$ ), before being subjected to recycling at  $C/20$  (rate capability test). The initial specific capacity delivered during first cycles at  $C/20$  approached 150  $\text{mAh g}^{-1}$ , which is close to the practical capacity delivered by the commercial LFP electrode cycled with standard LP30 liquid electrolyte (i.e.,  $\sim 158 \text{ mAh g}^{-1}$  at  $C/20$ ).<sup>38</sup> Excellent cycling stability was demonstrated with outstanding Coulombic efficiency (CE) close to 100% during the whole cycling test, as well as remarkable capacity retention of  $\sim 94\%$  after 25 cycles at different  $C$  rates. The inset of Figure 2a shows charge/discharge potential profiles versus specific capacity at different current rates, which perfectly resemble the typical flat plateaus of the LFP cathode corresponding to the  $\text{Li}^+$  ion

insertion (discharge) in the  $\text{FePO}_4$  network. The observed profiles remained stable even upon doubling the current rate, with overall limited overpotential that only slightly increased at a higher rate of  $C/5$ , supporting the favorable charge transport properties of the system.

A second Li-metal cell was assembled with the same configuration and tested for prolonged charge/discharge cycling. Results are remarkable and the cell delivered capacity values exceeding  $125 \text{ mAh g}^{-1}$  during initial cycling at a relatively high  $C$  rate of  $C/5$  (Figure 2b). The cycling performance of the similar cells based on copoly(LiMTFSI)<sup>22</sup> and copoly(LiMESTTFSI)<sup>25</sup> is shown in Figures S27 and S28 for comparison. It can be clearly observed that the replacement of an alkyl or ester spacer in the ionic monomer with the one based on  $-\text{EO}-$  units has drastically improved the battery performance in terms of capacity retention and the output at elevated charge/discharge rates. Indeed, the Li/coPIL2/LFP cell provided stable cycling at high Coulombic efficiency, being able to deliver specific capacity exceeding  $100 \text{ mAh g}^{-1}$  (with almost 65% capacity retention, see Figure 2), while the Li/copol(LiMTFSI)/LFP and Li/copol(LiMESTTFSI)/LFP cells provided specific capacity values limited to only 40 and  $35 \text{ mAh g}^{-1}$ , respectively, at the same cycling conditions (see Figures S27 and S28).

## CONCLUSION

In the present work, for the first time, the (trifluoromethane)-sulfonylimide anion was chemically bonded to the methacrylic reactive group through a flexible spacer containing 10 oxyethylene units. The synthesized TBAM(PEG)TFSI monomer readily underwent homo- and copolymerization with poly(ethylene glycol) methyl ether methacrylate to give solid polyelectrolytes with high molecular weight (up to  $M_n = 85\,900 \text{ g mol}^{-1}$ ). Simple free-radical homopolymerization of TBAM(PEG)TFSI and subsequent ion exchange to Li cations yielded the rubbery material  $-\text{PIL}$  that demonstrated ionic conductivity that was significantly higher, compared to its alkyl- or ester-based spacer previously developed analogues, namely, poly(LiMTFSI) and poly(LiMESTTFSI) ( $9.2 \times 10^{-8} \text{ S cm}^{-1}$  vs  $1.1 \times 10^{-12}$  and  $<10^{-11} \text{ S cm}^{-1}$  at  $25^\circ\text{C}$ , respectively). Further random copolymerization of TBAM(PEG)TFSI with PEGM in 1:1, 1:2, and 1:4 molar ratios was performed and followed by ion exchange with LiCl provided cold flowing rubber-like copolymers (viz., coPIL1–coPIL3) with enhanced ionic conductivity. Among tested copolymers, the coPIL2 provided the highest ionic conductivity in the whole range of examined temperatures ( $3.0 \times 10^{-6}$  and  $3.8 \times 10^{-5} \text{ S cm}^{-1}$  at  $25$  and  $70^\circ\text{C}$ , respectively), excellent compatibility with the Li metal electrode, electrochemical stability, and optimal viscoelastic behavior, allowing the fabrication of the truly solid-state laboratory-scale Li metal cells with LFP-based cathode. Such cells provided stable cycling, high rate capability, excellent Coulombic efficiency, and even sustained more than 200 cycles at a relatively high current rate ( $C/5$ ) at  $70^\circ\text{C}$  without any observable signs of short circuits and/or dendrite growth. After 200 charge/discharge cycles at the  $C/5$  rate, the cell was able to deliver the specific capacity close to  $100 \text{ mAh g}^{-1}$ , hence, outperforming previously reported similar Li-metal cells, based on copoly(LiMTFSI), poly(LiMESTTFSI), or other analogous SICPs.

To conclude, the most striking advantages of the developed SICPs on the basis of the novel ionic monomer TBAM(PEG)TFSI are (1) the low glass-transition temperatures ( $T_g$

values down to  $-50^\circ\text{C}$ ); (2) the high ionic conductivity (up to  $3.0 \times 10^{-6} \text{ S cm}^{-1}$  at  $25^\circ\text{C}$ ); (3) the thermal stability sufficient for LiMBs ( $T_{\text{onset}}$  of  $200^\circ\text{C}$ ); (4) the improved storage and loss moduli in comparison with known copoly(LiMTFSI) analogue; (5) good anodic electrochemical stability (up to  $4.5 \text{ V}$  vs  $\text{Li}^+/\text{Li}$  at  $70^\circ\text{C}$ ); (6) excellent Li ion transport resulting in a lithium-ion transference number close to unity ( $t_{\text{Li}^+} = 0.96\text{--}0.98$ ); (7) superior electrochemical features, which allowed stable cycling in Li/coPIL2/LFP cells with capacity outputs close to the LFP practical values and capacity retention at relatively high current charge/discharge rates, pointing out the relevance of this work in the development of next-generation SICPs to be exploited in practical high performing and safe truly solid-state LiMBs.

## ASSOCIATED CONTENT

### Supporting Information

The Supporting Information is available free of charge at <https://pubs.acs.org/doi/10.1021/acsmaterialslett.4c01647>.

Materials and methods, full experimental details for the synthesis of TBAM(PEG)TFSI monomer, homopolymer PIL and copolymers coPIL1–coPIL3, description of the characterization techniques for the determination of PEGM/LiM(PEG)TFSI ratio in copolymers,  $^1\text{H}$ ,  $^{13}\text{C}$ ,  $^{19}\text{F}$ , HSQC NMR, IR and GPC-ESI-HRMS spectra of TBAM(PEG)TFSI, DSC traces of TBAM(PEG)TFSI,  $^1\text{H}$ ,  $^7\text{Li}$ ,  $^{19}\text{F}$  NMR and IR spectra of PIL and coPIL1–coPIL3, DSC and TGA traces of copolymers, electrochemical stability window of coPIL2 obtained by CV at  $70^\circ\text{C}$ , EIS and polarization current curves of coPIL2 in Li/coPIL2/Li configuration, charge transfer-resistance ( $R_{\text{ct}}$ ) at the electrolyte/electrode interface of cell with Li/coPIL2/Li configuration at  $70^\circ\text{C}$ , charge interfacial resistance variation over time in a laboratory-scale Li metal cell with Li/coPIL2/Li configuration at  $70^\circ\text{C}$  (PDF)

## AUTHOR INFORMATION

### Corresponding Authors

Claudio Gerbaldi – GAME Lab, Department of Applied Science and Technology (DISAT), Politecnico di Torino, 10129 Torino, Italy; National Reference Center for Electrochemical Energy Storage (GISEL), 50121 Firenze, Italy; [orcid.org/0000-0002-8084-0143](https://orcid.org/0000-0002-8084-0143); Email: [claudio.gerbaldi@polito.it](mailto:claudio.gerbaldi@polito.it)

Alexander S. Shaplov – Luxembourg Institute of Science and Technology (LIST), L-4362 Esch-sur-Alzette, Luxembourg; [orcid.org/0000-0002-7789-2663](https://orcid.org/0000-0002-7789-2663); Email: [alexander.shaplov@list.lu](mailto:alexander.shaplov@list.lu)

### Authors

Gabriele Lingua – GAME Lab, Department of Applied Science and Technology (DISAT), Politecnico di Torino, 10129 Torino, Italy; National Reference Center for Electrochemical Energy Storage (GISEL), 50121 Firenze, Italy; POLYMAT, University of the Basque Country UPV/EHU, 20018 Donostia-San Sebastian, Spain; [orcid.org/0000-0002-9878-0185](https://orcid.org/0000-0002-9878-0185)

Vladislav Y. Shevtsov – Luxembourg Institute of Science and Technology (LIST), L-4362 Esch-sur-Alzette, Luxembourg; Department of Physics and Materials Science, University of



Luxembourg, L-4365 Esch-sur-Alzette, Luxembourg;

orcid.org/0000-0002-9373-5270

**Petr S. Vlasov** – Department of Macromolecular Chemistry, Saint-Petersburg State University, 198504 Saint-Petersburg, Russia; Present Address: FaradaIC Sensors GmbH, Berlin, Germany

**Laura Puchot** – Luxembourg Institute of Science and Technology (LIST), L-4362 Esch-sur-Alzette, Luxembourg

Complete contact information is available at:

<https://pubs.acs.org/10.1021/acsmaterialslett.4c01647>

## Author Contributions

<sup>†</sup>Dr. G. Lingua and V. Y. Shevtsov contributed equally to this work. The manuscript was written through contributions of all authors. All authors have given approval to the final version of the manuscript. CRediT: **Gabriele Lingua** data curation, investigation, writing - original draft, writing - review & editing; **Vladislav Y. Shevtsov** conceptualization, investigation, writing - original draft; **Petr S. Vlasov** data curation, investigation, validation, writing - original draft; **Laura Puchot** data curation, investigation, writing - original draft; **Claudio Gerbaldi** conceptualization, data curation, funding acquisition, methodology, supervision, writing - original draft, writing - review & editing; **Alexander S. Shaplov** conceptualization, funding acquisition, investigation, methodology, supervision, writing - original draft, writing - review & editing.

## Funding

This work was in part supported by Luxembourg National Research Fund (FNR) through FNRS-FNR INTER project INFINITE (Agreement No. INTER/FNRS/21/16555380/INFINITE), in part by the PSIONIC project, which has received funding from the European Union's Horizon Europe Research and Innovation Programme under Grant Agreement N. 101069703.

## Notes

The authors declare no competing financial interest.

## ACKNOWLEDGMENTS

The PSIONIC project has received funding from the European Union's Horizon Europe Research and Innovation Programme under Grant Agreement N. 101069703. G. Lingua is grateful to the Luxembourg Institute of Science and Technology (LIST) for the sponsorship of his visit and work in the Materials and Research Technology Department (MRT). Authors would like to acknowledge the support of MOST–Sustainable Mobility Center and received funding from the European Union Next-GenerationEU (PIANO NAZIONALE DI RIPRESA E RESILIENZA–PNRR e MISSIONE 4 COMPONENTE 2, INVESTIMENTO 1.4 e D.D. 1033 June 17, 2022, CN00000023, Spoke 13 - POC Hyless). This manuscript reflects only the authors' views and opinions, and neither the European Union nor the European Commission can be considered responsible for them.

## REFERENCES

- (1) Zhang, H.; Li, C.; Piszcz, M.; Coya, E.; Rojo, T.; Rodriguez-Martinez, L. M.; Armand, M.; Zhou, Z. Single Lithium-Ion Conducting Solid Polymer Electrolytes: Advances and Perspectives. *Chem. Soc. Rev.* **2017**, *46* (3), 797–815.
- (2) Eshetu, G. G.; Mecerreyes, D.; Forsyth, M.; Zhang, H.; Armand, M. Polymeric Ionic Liquids for Lithium-Based Rechargeable Batteries. *Mol. Syst. Des. Eng.* **2019**, *4* (2), 294–309.
- (3) Bannister, D. J.; Davies, G. R.; Ward, I. M.; McIntyre, J. E. Ionic Conductivities for Poly(Ethylene Oxide) Complexes with Lithium Salts of Monobasic and Dibasic Acids and Blends of Poly(Ethylene Oxide) with Lithium Salts of Anionic Polymers. *Polymer (Guildf)* **1984**, *25* (9), 1291–1296.
- (4) Shaplov, A. S.; Vlasov, P. S.; Armand, M.; Lozinskaya, E. I.; Ponkratov, D. O.; Malyshkina, I. A.; Vidal, F.; Okatova, O. V.; Pavlov, G. M.; Wandrey, C.; Godovikov, I. A.; Vygotskii, Y. S. Design and Synthesis of New Anionic “Polymeric Ionic Liquids” with High Charge Delocalization. *Polym. Chem.* **2011**, *2* (11), 2609–2618.
- (5) Porcarelli, L.; Shaplov, A. S.; Salsamendi, M.; Nair, J. R.; Vygotskii, Y. S.; Mecerreyes, D.; Gerbaldi, C. Single-Ion Block Copoly(Ionic Liquid)s as Electrolytes for All-Solid State Lithium Batteries. *ACS Appl. Mater. Interfaces* **2016**, *8* (16), 10350–10359.
- (6) Meziane, R.; Bonnet, J. P.; Courty, M.; Djellab, K.; Armand, M. Single-Ion Polymer Electrolytes Based on a Delocalized Polyanion for Lithium Batteries. *Electrochim. Acta* **2011**, *57* (1), 14–19.
- (7) Bouchet, R.; Maria, S.; Meziane, R.; Aboulaich, A.; Lienafa, L.; Bonnet, J. P.; Phan, T. N. T.; Bertin, D.; Gigmes, D.; Devaux, D.; Denoyel, R.; Armand, M. Single-Ion BAB Triblock Copolymers as Highly Efficient Electrolytes for Lithium-Metal Batteries. *Nat. Mater.* **2013**, *12* (5), 452–457.
- (8) Jeong, K.; Park, S.; Lee, S. Y. Revisiting Polymeric Single Lithium-Ion Conductors as an Organic Route for All-Solid-State Lithium Ion and Metal Batteries. *J. Mater. Chem. A* **2019**, *7* (5), 1917–1935.
- (9) Doyle, M.; Fuller, T. F.; Newman, J. The Importance of the Lithium Ion Transference Number in Lithium/Polymer Cells. *Electrochim. Acta* **1994**, *39* (13), 2073–2081.
- (10) Shaplov, A. S.; Marcilla, R.; Mecerreyes, D. Recent Advances in Innovative Polymer Electrolytes Based on Poly(Ionic Liquid)s. *Electrochim. Acta* **2015**, *175*, 18–34.
- (11) Xue, Z.; He, D.; Xie, X. Poly(Ethylene Oxide)-Based Electrolytes for Lithium-Ion Batteries. *J. Mater. Chem. A* **2015**, *3* (38), 19218–19253.
- (12) Liu, Y.; Zhang, Y.; Pan, M.; Liu, X.; Li, C.; Sun, Y.; Zeng, D.; Cheng, H. A Mechanically Robust Porous Single Ion Conducting Electrolyte Membrane Fabricated via Self-Assembly. *J. Membr. Sci.* **2016**, *507*, 99–106.
- (13) Chen, Y.; Ke, H.; Zeng, D.; Zhang, Y.; Sun, Y.; Cheng, H. Superior Polymer Backbone with Poly(Arylene Ether) over Polyamide for Single Ion Conducting Polymer Electrolytes. *J. Membr. Sci.* **2017**, *525*, 349–358.
- (14) Nguyen, H. D.; Kim, G. T.; Shi, J.; Paillard, E.; Judeinstein, P.; Lyonard, S.; Bresser, D.; Jojoiu, C. Nanostructured Multi-Block Copolymer Single-Ion Conductors for Safer High-Performance Lithium Batteries. *Energy Environ. Sci.* **2018**, *11* (11), 3298–3309.
- (15) Luo, G.; Yuan, B.; Guan, T.; Cheng, F.; Zhang, W.; Chen, J. Synthesis of Single Lithium-Ion Conducting Polymer Electrolyte Membrane for Solid-State Lithium Metal Batteries. *ACS Appl. Energy Mater.* **2019**, *2* (5), 3028–3034.
- (16) Cao, P. F.; Li, B.; Yang, G.; Zhao, S.; Townsend, J.; Xing, K.; Qiang, Z.; Vogiatzis, K. D.; Sokolov, A. P.; Nanda, J.; Saito, T. Elastic Single-Ion Conducting Polymer Electrolytes: Toward a Versatile Approach for Intrinsically Stretchable Functional Polymers. *Macromolecules* **2020**, *53* (9), 3591–3601.
- (17) Jangu, C.; Savage, A. M.; Zhang, Z.; Schultz, A. R.; Madsen, L. A.; Beyer, F. L.; Long, T. E. Sulfonimide-Containing Triblock Copolymers for Improved Conductivity and Mechanical Performance. *Macromolecules* **2015**, *48* (13), 4520–4528.
- (18) Inceoglu, S.; Rojas, A. A.; Devaux, D.; Chen, X. C.; Stone, G. M.; Balsara, N. P. Morphology-Conductivity Relationship of Single-Ion-Conducting Block Copolymer Electrolytes for Lithium Batteries. *ACS Macro Lett.* **2014**, *3* (6), 510–514.
- (19) Rojas, A. A.; Inceoglu, S.; Mackay, N. G.; Thelen, J. L.; Devaux, D.; Stone, G. M.; Balsara, N. P. Effect of Lithium-Ion Concentration on Morphology and Ion Transport in Single-Ion-Conducting Block Copolymer Electrolytes. *Macromolecules* **2015**, *48* (18), 6589–6595.



- (20) Thelen, J. L.; Inceoglu, S.; Venkatesan, N. R.; Mackay, N. G.; Balsara, N. P. Relationship between Ion Dissociation, Melt Morphology, and Electrochemical Performance of Lithium and Magnesium Single-Ion Conducting Block Copolymers. *Macromolecules* **2016**, *49* (23), 9139–9147.
- (21) Devaux, D.; Liénafa, L.; Beaudoin, E.; Maria, S.; Phan, T. N. T.; Gigmes, D.; Giroud, E.; Davidson, P.; Bouchet, R. Comparison of Single-Ion-Conductor Block-Copolymer Electrolytes with Polystyrene-TFSI and Polymethacrylate-TFSI Structural Blocks. *Electrochim. Acta* **2018**, *269*, 250–261.
- (22) Lingua, G.; Grysan, P.; Vlasov, P. S.; Verge, P.; Shaplov, A. S.; Gerbaldi, C. Unique Carbonate-Based Single Ion Conducting Block Copolymers Enabling High-Voltage, All-Solid-State Lithium Metal Batteries. *Macromolecules* **2021**, *54* (14), 6911–6924.
- (23) Porcarelli, L.; Aboudzadeh, M. A.; Rubatat, L.; Nair, J. R.; Shaplov, A. S.; Gerbaldi, C.; Mecerreyes, D. Single-Ion Triblock Copolymer Electrolytes Based on Poly(Ethylene Oxide) and Methacrylic Sulfonamide Blocks for Lithium Metal Batteries. *J. Power Sources* **2017**, *364*, 191–199.
- (24) Lozinskaya, E. I.; Ponkratov, D. O.; Malyshkina, I. A.; Grysan, P.; Lingua, G.; Gerbaldi, C.; Shaplov, A. S.; Vygodskii, Y. S. Self-Assembly of Li Single-Ion-Conducting Block Copolymers for Improved Conductivity and Viscoelastic Properties. *Electrochim. Acta* **2022**, *413*, No. 140126.
- (25) Porcarelli, L.; Vlasov, P. S.; Ponkratov, D. O.; Lozinskaya, E. I.; Antonov, D. Y.; Nair, J. R.; Gerbaldi, C.; Mecerreyes, D.; Shaplov, A. S. Design of Ionic Liquid like Monomers towards Easy-Accessible Single-Ion Conducting Polymer Electrolytes. *Eur. Polym. J.* **2018**, *107*, 218–228.
- (26) Ma, Q.; Zhang, H.; Zhou, C.; Zheng, L.; Cheng, P.; Nie, J.; Feng, W.; Hu, Y. S.; Li, H.; Huang, X.; Chen, L.; Armand, M.; Zhou, Z. Single Lithium-Ion Conducting Polymer Electrolytes Based on a Super-Delocalized Polyanion. *Angew. Chem., Int. Ed.* **2016**, *55* (7), 2521–2525.
- (27) Rohan, R.; Pareek, K.; Chen, Z.; Cai, W.; Zhang, Y.; Xu, G.; Gao, Z.; Cheng, H. A High Performance Polysiloxane-Based Single Ion Conducting Polymeric Electrolyte Membrane for Application in Lithium Ion Batteries. *J. Mater. Chem. A* **2015**, *3* (40), 20267–20276.
- (28) Ikeda, T. Anionic Glycidyl Triazolyl Polymers: Oppositely Charged Analogs of Imidazolium-Based Cationic Glycidyl Triazolyl Polymers. *Macromolecules* **2023**, *56* (22), 9229–9236.
- (29) Jüger, J.; Meyer, F.; Vidal, F.; Chevrot, C.; Teyssié, D. Synthesis, Polymerization and Conducting Properties of an Ionic Liquid-Type Anionic Monomer. *Tetrahedron Lett.* **2009**, *50* (1), 128–131.
- (30) Ho, H. T.; Rollet, M.; Phan, T. N. T.; Gigmes, D. Michael Addition Reaction onto Vinyl Sulfonyl(Trifluoromethylsulfonyl)-Imide: An Easy Access to Sulfonyl(Trifluoromethylsulfonyl)Imide-Based Monomers and Polymers. *Eur. Polym. J.* **2018**, *107*, 74–81.
- (31) Matsumoto, K.; Endo, T. Preparation and Properties of Ionic-Liquid-Containing Poly(Ethylene Glycol)-Based Networked Polymer Films Having Lithium Salt Structures. *J. Polym. Sci. Part A Polym. Chem.* **2011**, *49* (16), 3582–3587.
- (32) Jüger, J.; Vancaeyzeele, C.; Plesse, C.; Nguyen, G. M. T.; Ribeiro, F. B.; Teyssié, D.; Vidal, F. Polymeric Ionic Liquid Based Interpenetrating Polymer Network for All-Solid Self-Standing Polyelectrolyte Material. *Eur. Polym. J.* **2018**, *106*, 257–265.
- (33) Nguyen, G. T. M.; Michan, A. L.; Fannir, A.; Viallon, M.; Vancaeyzeele, C.; Michal, C. A.; Vidal, F. Self-Standing Single Lithium Ion Conductor Polymer Network with Pendant Trifluoromethanesulfonylimide Groups: Li<sup>+</sup> Diffusion Coefficients from PFGSTE NMR. *Eur. Polym. J.* **2013**, *49* (12), 4108–4117.
- (34) Porcarelli, L.; Sutton, P.; Bocharova, V.; Aguirresarobe, R. H.; Zhu, H.; Goujon, N.; Leiza, J. R.; Sokolov, A.; Forsyth, M.; Mecerreyes, D. Single-Ion Conducting Polymer Nanoparticles as Functional Fillers for Solid Electrolytes in Lithium Metal Batteries. *ACS Appl. Mater. Interfaces* **2021**, *13* (45), 54354–54362.
- (35) Porcarelli, L.; Manojkumar, K.; Sardon, H.; Llorente, O.; Shaplov, A. S.; Vijayakrishna, K.; Gerbaldi, C.; Mecerreyes, D. Single Ion Conducting Polymer Electrolytes Based On Versatile Polyurethanes. *Electrochim. Acta* **2017**, *241*, 526–534.
- (36) Evans, J.; Vincent, C. A.; Bruce, P. G. Electrochemical Measurement of Transference Numbers in Polymer Electrolytes. *Polymer (Guildford)* **1987**, *28* (13), 2324–2328.
- (37) Abraham, K. M.; Jiang, Z.; Carroll, B. Highly Conductive PEO-like Polymer Electrolytes. *Chem. Mater.* **1997**, *9* (9), 1978–1988.
- (38) Metzger, M.; Sicklinger, J.; Haering, D.; Kavakli, C.; Stinner, C.; Marino, C.; Gasteiger, H. A. Carbon Coating Stability on High-Voltage Cathode Materials in H<sub>2</sub>O-Free and H<sub>2</sub>O-Containing Electrolyte. *J. Electrochem. Soc.* **2015**, *162* (7), A1227–A1235.